Analyses of Shuttle Orbiter Approach and Landing

Irving L. Ashkenas,* Roger H. Hoh,† and Gary L. Teper‡
Systems Technology, Inc., Hawthorne, California

This paper summarizes a study of the Shuttle Orbiter approach and landing conditions. Causes of observed pilot-induced oscillation tendencies are identified and potential cures are examined. Closed-loop pilot/vehicle analyses are described and path/attitude stability boundaries defined. The latter novel approach proved of great value in delineating and illustrating the basic causes of this multiloop pilot control problem. The analytical results are shown to be consistent with flight test and fixed-base simulation. Conclusions are drawn relating to possible improvements of the Shuttle Orbiter/digital flight control systems.

Nomenclature

h = altitude
h_p = altitude at pilot's location
h_{p_c} = commanded pilot's altitude
h_{p_e} = pilots altitude error, $h_{p_c} - h_p$
K = open-loop gain
K_{ph} = pilot gain of outer altitude loop
$K_{p\theta}$ = pilot gain of inner attitude loop
$K_{\theta\delta_e}$ = pitch attitude to elevator gain
$N^h_{\delta_e}$ = numerator of altitude to elevator transfer function
$N^\theta_{\delta_e}$ = pitch attitude to elevator numerator
s = Laplace transform variable, $s = \sigma \pm j\omega$
T_E = first-order time constant for low-order equivalent system
T_{h1}, T_{h2}, T_{h3} = time constants, altitude numerator
T_{L_θ} = pilot lead time constant of inner attitude loop
$T_{\theta 1}, T_{\theta 2}$ = time constants, pitch attitude numerator
Y_{ph} = pilot describing function operating on path deviation
$Y_{p\theta}$ = pilot model describing function operating on attitude
δ_s = control stick deflection
δ_e = elevator surface deflection
θ = pitch attitude (perturbation)
θ_c = pitch attitude command
θ_e = pitch attitude error
τ = time delay
τ_e = effective pilot time delay
τ_p = phase delay
τ_θ = pilot time delay applicable to inner attitude loop
$\omega_{c\theta}$ = inner-loop crossover frequency
ω_h, ζ_h = altitude to elevator numerator frequency, damping ratio
ω_{sp} = short-period frequency
$( )'$ = quantities/characteristics modified by a single-loop closure
$( )''$ = quantities/characteristics modified by two successive loop closures

Introduction

IN November 1978, a study program was initiated to: "Conduct independent analyses of the Shuttle Orbiter approach and landing conditions to ascertain possible causes and potential cures for observed PIO-like flight deficiencies."[1]

The deficiencies caused by pilot-induced oscillations (PIO) were observed at the end of the Space Shuttle Orbiter Approach and Landing Test (ALT) Program,[2,3] Oct. 26, 1977, when free-flight 5 (FF5) was manually flown to a landing on concrete runway 04 at Edwards Air Force Base, California. This paper summarizes the work accomplished and the results presented at the Shuttle Landing Workshop held at NASA Johnson Space Center, Houston, in March 1979.

The phases of the technical approach used in the study were as follows:

1) Identification and quantification of the PIO cause. This was accomplished by examination of the PIO flight evidence and application of closed-loop pilot/vehicle analyses. Critical quantitative features of the PIO were identified and approximately reproduced analytically. Definition of closed-loop path/attitude stability boundaries was determined to be a valuable technique for delineating and illustrating the basic causes of this particular PIO.

2) Comparison of pilot control characteristics of the Orbiter with a "good" aircraft. The same analytic techniques used for the Orbiter were applied to the YF-12 that had flown the Orbiter approach and landing task without problems. Comparison of the Orbiter and YF-12 control characteristics allowed the identification of critical differences. A limited manned real-time simulation confirmed that the analytically exposed differences correlated with overall path/attitude control qualities.

3) Delineation and examination of potential improvements. Flight control system modifications that could improve critical Orbiter control characteristics were examined and analytically evaluated. The limited manned simulation was used to evaluate the effectiveness of potential conventional control system modifications. A preliminary assessment of the effects of surface rate limiting and attempts to minimize them through the use of a novel nonlinear stick filter ("PIO suppression filter") were also accomplished.

Presented as Paper 82-1607 at the AIAA Guidance and Control, Atmospheric Flight Mechanics, and Astrodynamics Conference, San Diego, Calif., Aug. 9-11, 1982; submitted Aug. 9, 1982; revision received June 7, 1983.

*Technical Director. Fellow AIAA.
†Principal Research Engineer. Associate Fellow AIAA.
‡Currently Research Department Manager, Sperry/Systems Management—Secor, Fairfax, Va. Associate Fellow AIAA.

Identification and Quantification of the PIO Cause

Time histories from ALT-FF5 are presented first and critical features of the PIO are noted. The pilot/vehicle analyses that successfully reproduced the salient FF5 phenomena are then described and discussed.

Free Flight 5: Flight Evidence of the PIO

Pertinent time histories from FF5 for approximately 12 s prior to first touchdown are shown in Fig. 1. The figure includes the pilot's input, i.e., the rotational hand controller (RHC) pitch deflection, "elevator" (longitudinal elevon) pitch rate, and altitude signals.

Examination of the time histories indicates that two modes were involved in the PIO. A higher frequency mode, which has been designated as $\omega''_{sp} = 3.4$ rad/s, is clearly evident in the pitch rate, elevator, and RHC responses. A lower frequency mode, designated as $\omega''_h = 1.9$ rad/s, is apparent in the altitude response. The existence of both modes, which were approximately neutrally stable for the last 8-10 s prior to first touchdown, is a crucial aspect of the observed PIO situation, as will later be discussed.

There is evidence of some elevator surface rate limiting in the responses shown in Fig. 1 and also in other flight test data not presented. The analyses given below and the simulation described later are consistent with the conclusion that rate limiting played a significant, but not crucial role, in the ALT-FF5 pitch PIO.

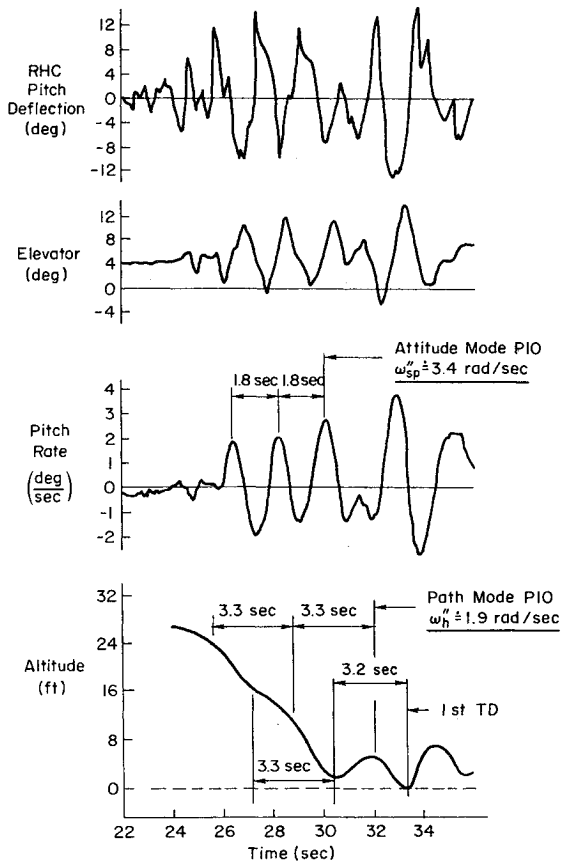

Fig. 1 FF5 flight evidence of PIO.

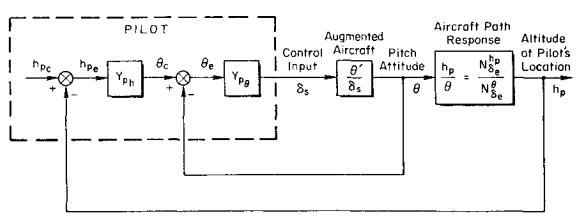

Fig. 2 Control structure for pilot/vehicle analyses.

Approach and Landing Closed-Loop Analysis

The quasilinear human pilot model of Ref. 4 was applied to the ALT-FF5 approach and landing flight condition. The control structure, pilot model form, and pilot model parameter values were based on existing flight test and simulator results.[4,5]

Control Structure

The control structure is presented in the block diagram of Fig. 2. The primary guidance requirement in the landing approach task is to maintain the desired path, i.e., altitude. The control structure shown reflects a pilot technique for controlling aircraft attitude in proportion to pilot-perceived altitude errors. The inner-attitude loop, as thus utilized, provides equalization (i.e., lead) for the outer-path loop; it also recognizes the additional task requirement of maintaining attitude control per se.

Aircraft Characteristics

The pertinent aircraft characteristics are represented by the two right-hand blocks in Fig. 2, i.e.,

θ'/δ_s = augmented pitch attitude transfer function for control inputs

h_p/θ = aircraft's path response to attitude changes for pilot contol inputs

This representation of the aircraft dynamics as a two-block series is consistent with the Orbiter's single control point. It is also very useful, as discussed further below, to delineate and emphasize the relevant aircraft characteristics.

The ALT-FF5 pitch attitude transfer function and frequency response are given in Fig. 3. Also given in the figure are the transfer function and frequency response of a low-order "equivalent" system model of the form,

$$\left.\frac{\theta}{\delta_s}\right]'_{eq} = \frac{Ke^{-\tau_e s}}{s(T_E s+1)}$$

and parameter values ($K = 0.4$ deg/s/deg, $1/T_E = 3.5$ rad/s, and $\tau_e = 0.264$ s) giving a best fit to the complete frequency response of the ALT. The equivalent system is useful for selecting pilot model parameter values and for making comparisons with other aircraft. The actual PIO analysis used the complete ALT transfer function as given in Fig. 3.

The path to attitude transfer function and frequency response for elevator inputs is

$$\frac{h_p}{\theta} = \frac{N^{h_p}_{\delta_e}}{N^{\theta}_{\delta_e}} = \frac{K_{h_p}\delta_e (s+1/T_{h_1})(s+1/T_{h_2})(s+1/T_{h_3})}{K_{\theta_{\delta_e}}(s+1/T_{\theta_1})(s+1/T_{\theta_2})}$$

$$= \frac{-2.25(s+0.026)(s+4.45)(s-4.91)}{s(s+0.042)(s+0.72)}$$

It should be recognized that these characteristics are identical to the unaugmented airframe and cannot be modified by feedbacks or feedforwards to the elevator.

Only the above higher frequency roots (i.e., $1/T_{\theta_2}$, $1/T_{h_2}$, and $1/T_{h_3}$) are of concern to the PIO problems. Their values are set by basic airframe characteristics. T_{θ_2}, the flight path lag, is due to wing loading and C_{L_α}; T_{h_2} and T_{h_3} are set primarily by the pilot's location relative to the center of instantaneous rotation (CIR) for elevator inputs. For a pilot location aft of the CIR, as in the Orbiter, $1/T_{h_2}$ and $1/T_{h_3}$ will be two distinct first-order roots of approximately the same magnitude but of opposite sign. In aircraft where the pilot is located forward of the CIR (the more common case), these two roots will couple into a second-order pair ω_h. This is

illustrated later, where the Orbiter characteristics are compared to other aircraft. For a more complete discussion of these transfer functions and approximations for the values of their roots, see Ref. 6.

Pilot Characteristics

The other half of the Fig. 2 block diagram, representing the pilot's characteristics, consists of the two left-hand blocks enclosed within the dashed box. Y_{p_θ} accounts for the pilot's action in closing the inner attitude-to-elevator loop; Y_{p_h} accounts for his closure of the outer path-to-attitude loop. The pilot model forms used in the analysis are

$$Y_{p_\theta} = K_{p_\theta}(T_{L_\theta}s+1)e^{-\tau_\theta s}$$

$$Y_{ph} = K_{p_h}$$

The inner-loop pilot model describing function Y_{p_θ} accounts for the pilot's gain K_{p_θ}, lead T_{L_θ}, and time delay τ_θ in controlling attitude with elevator. The pilot will adjust his control characteristics for the particular vehicle and task at hand. As described in Ref. 4, the cardinal adjustment will be to create a "K/s region" in the frequency domain around "crossover." For attitude control, the important frequency region is typically from 0.5 to, say, 6.0 rad/s. Closed-loop performance, both in terms of average errors and time to make a steady-state correction, is improved by higher crossover frequencies. When only attitude control is the task and tight regulation is not required, the pilot can operate at the lower end of the above frequency region. As the attitude task becomes more stringent and/or an outer loop (such as altitude control) is added, he will have to operate at a higher crossover, say, 3.0 rad/s. If tight control, i.e., quick corrections, of outer-loop altitude errors is demanded, the equalization role of the inner loop will push attitude crossover to the higher end of the frequency region.

The lead term T_{L_θ} in the pilot model form is the means by which the model reflects the pilot's adjustment to create a K/s region, i.e., a rate response. Setting the lead equal to the Fig. 3 equivalent system lag achieves the desired result, as shown in the open-loop pilot/vehicle frequency response plot of Fig. 4b. By comparing this plot with the vehicle-alone characteristics in Fig. 3, it can be seen that the pilot's equalization has stretched the high end of the K/s region (i.e., corresponding to an amplitude response slope of -20 dB/decade) from about 1.0 rad/s to, say, 4.0 rad/s.

The pilot's time delay τ_θ, also included in the Fig. 4 system survey, has been shown[4] to be a function of the lead adopted; the relationship used herein is given by

$$\tau_\theta = \tau_e - 0.1$$

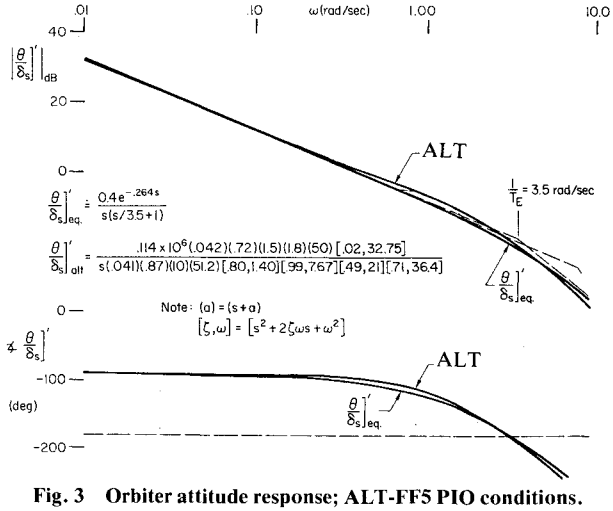

Fig. 3 Orbiter attitude response; ALT-FF5 PIO conditions.

to account for in-flight motion cues, and

$$1/\tau_e = 0.24 + 0.214\,(1/T_{L_\theta})$$

The use of a low-frequency pure gain pilot model K_{p_h} in the outer altitude loop is consistent with the experimental results of Ref. 7 and the analytical considerations of Ref. 8.

Pilot/Vehicle Closed-Loop Characteristics

For pilot attitude gains corresponding to crossover frequencies of 2.5-4.0 rad/s, the location of the closed-loop attitude mode ω'_{sp} is shown (as diamonds) in the root locus plot of Fig. 4a. As can be seen, the maximum stable crossover frequency is slightly less than 3.5 rad/s. The other critical mode shown in this plot is the path mode $1/T'_{\theta_2}$, which for the above range of pilot gains is very close to the basic aircraft flight path lag $1/T_{\theta_2}$.

These two inner-loop characteristics, ω'_{sp} and $1/T'_{\theta_2}$, limit outer-loop performance, as illustrated by the Fig. 5 root locus plots for pilot closure of the path loop. (Successive sets of diamond symbols along the three loci in each plot correspond to given increasing altitude gains.) These plots are for the three indicated levels of inner-loop crossover frequency. The top plot, for modest inner-loop gain, shows the stable attitude mode ω'_{sp} being further stabilized with increasing outer-loop gain resulting in the final closed-loop attitude mode designated by ω''_{sp}. The closed-loop path mode ω''_h results from the coupling of the $1/T'_{\theta_2}$ path mode and the kinematic altitude integration. The top plot also shows that, for modest inner-loop gain, the maximum stable path mode frequency is limited to about 1.4 rad/s. To achieve better path control, i.e., higher closed-loop bandwidth, the pilot must exercise tighter attitude control. That is, the middle Fig. 5 root locus shows that for increased inner-loop crossover (which incidentally yields near-neutral stability of the attitude mode without the outer loop), the achievable, stable path mode frequency has been increased to about 1.8 rad/s. For

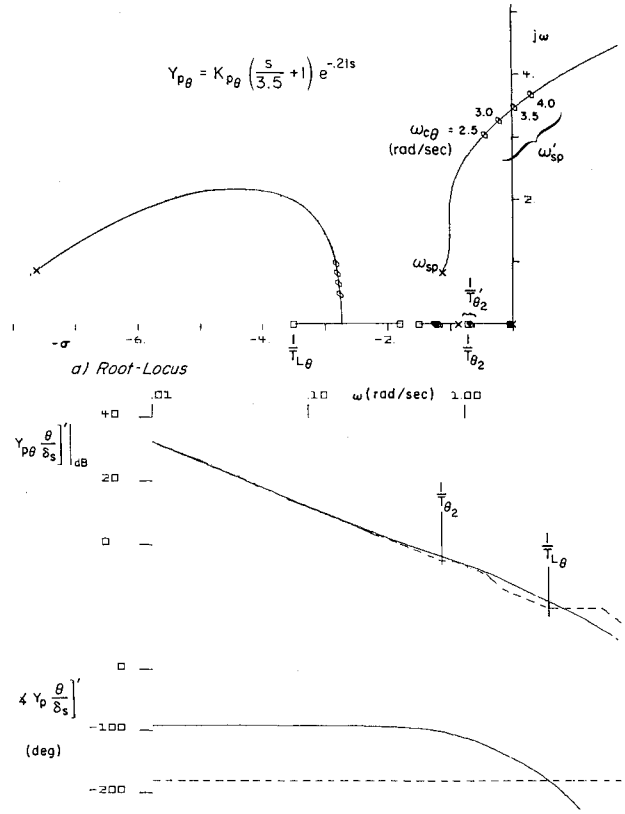

Fig. 4 System survey for pilot closure of attitude loop, Orbiter ALT configuration.

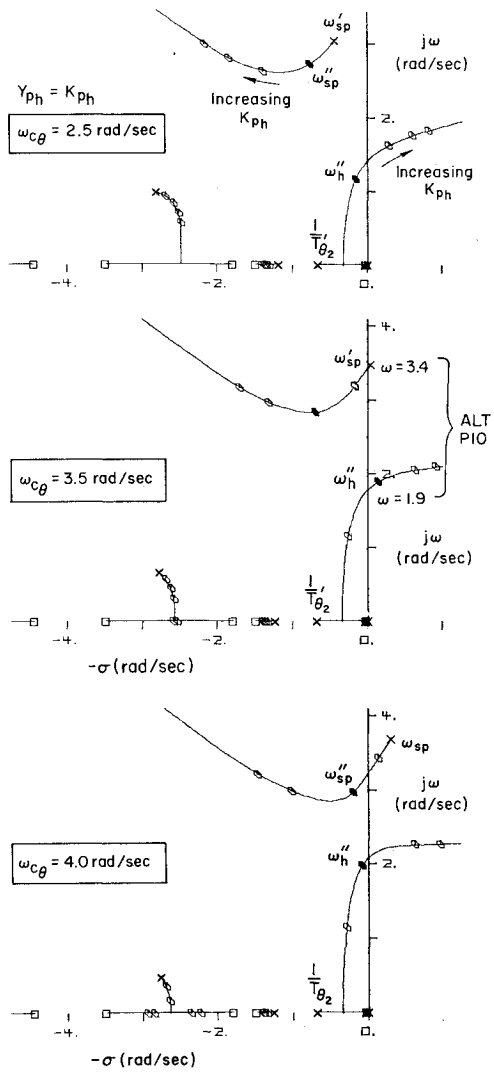

Fig. 5 Pilot closure of path loop, Orbiter ALT configuration.

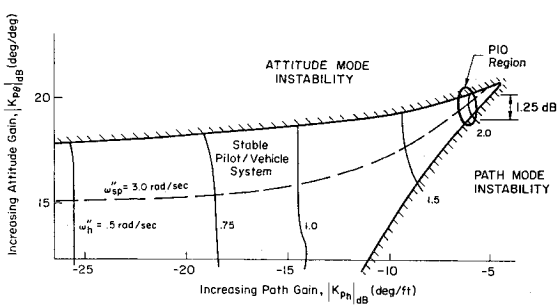

Fig. 6 Closed-loop path/attitude stability boundaries, pilot/ALT system.

reference, the observed ALT-FF5 PIO frequencies are noted in the center plot. The bottom plot illustrates that for higher inner-loop gain a minimum level of outer-loop gain is necessary to stabilize the attitude mode, but the potential improvement in path bandwidth is minimal.

The tradeoff between performance and stability is illustrated by the closed-loop path/attitude stability boundaries shown in Fig. 6. The figure shows the closed-loop stability limits as a function of combinations of attitude and path gain. Within the stable region, lines of constant closed-loop mode frequency are also shown. At lower attitude gains a path mode instability will result at the limiting path gain. Since the (right-hand) path mode boundary is sloping upward to the right, higher path gains resulting in better performace (higher ω''_h) can be achieved by increasing inner-loop attitude gain. This is true for attitude gains up to about 18 dB, which corresponds to an inner-loop crossover frequency of $\omega_{c_\theta} = 3.5$ rad/s (the middle plot in Fig. 5). As attitude gains increase beyond 18 dB, increasing levels of path gain are required to stabilize the attitude mode.

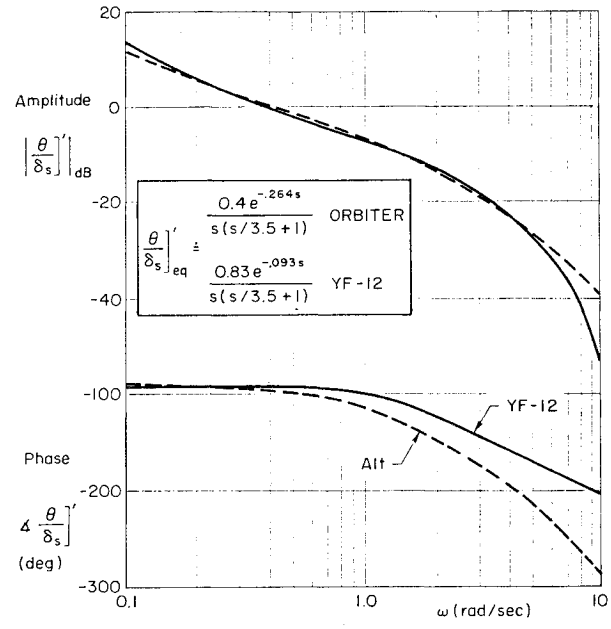

Fig. 7 Comparison of YF-12 and Orbiter attitude response, $\theta/\delta_s]'$.

For maximum performance, the pilot is drawn into the tip of the plot where the PIO region has been noted. At a stable operating point within this region, the system is very sensitive to both attitude and path gains. At a fixed attitude gain, lower path gain will result in an attitude mode instability, while a higher path gain results in a path mode instability. The range of stable path gains is only about 1.2 dB. A similar situation exists for fixed path gain. A higher attitude gain will result in an attitude mode instability and lower attitude gain in an unstable path mode. The only way to back out of this region in a stable manner is by a judicious, *simultaneous,* and peculiarly proportional reduction in both attitude and path gains, a very difficult if not impossible piloting task for an unexpectedly encountered PIO. This extreme sensitivity to small increases or decreases in individual pilot control characteristics is the essence of this particular PIO situation. Nonlinearities, e.g., due to elevon surface rate limiting, will accentuate but not otherwise alter this essential character. The existence in the ALT-FF5 flight test data of both neutrally stable modes at very nearly the same frequencies indicated by the analyses is strong evidence that we have analytically reproduced the PIO conditions.

Comparisons with a "Good" Aircraft

The above-described analytic procedure was applied to the YF-12, which has flown the Orbiter approach and landing task without problems, using aircraft data provided by the Dryden Flight Research Facility.

Aircraft Characteristics

As indicated in the preceding, the critical aircraft characteristics reside in the augmented attitude response to control inputs and the basic airframe path response to attitude

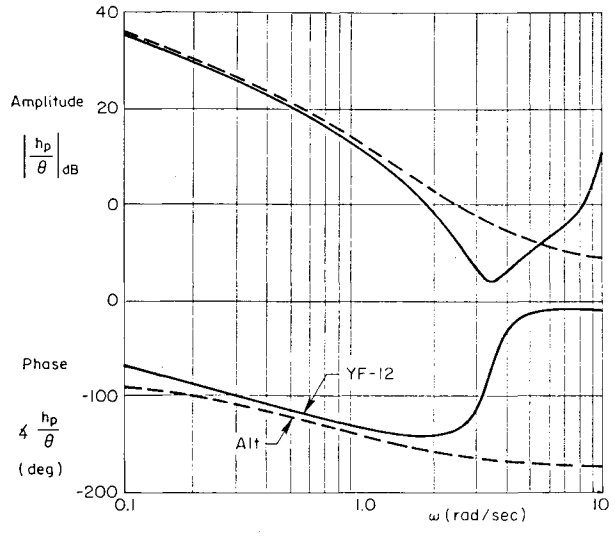

Fig. 8 Comparison of YF-12 and Orbiter path response, h_p/θ.

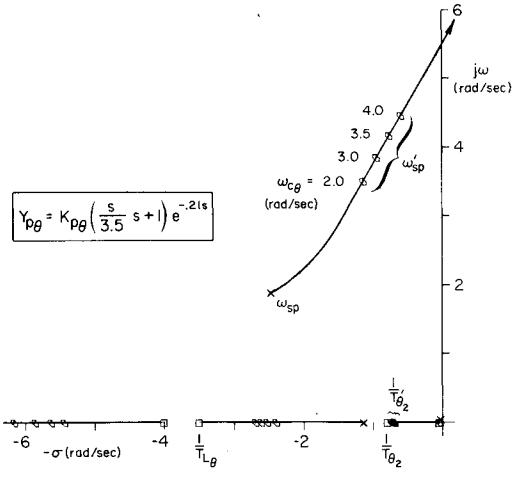

Fig. 9 Pilot closure of YF-12 attitude loop, θ!δ_s.

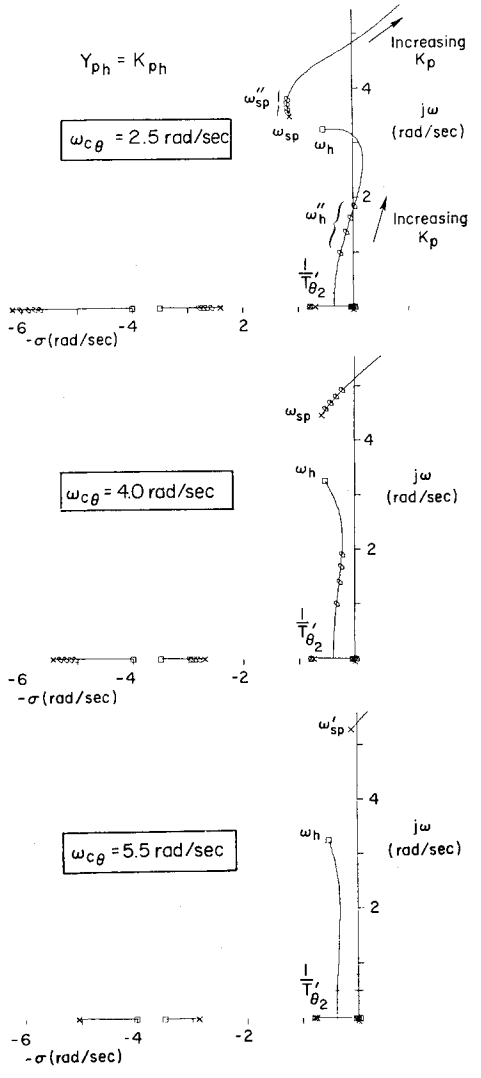

Fig. 10 Pilot closure of YF-12 path loop, $h_p \rightarrow \theta_c$.

changes. A comparison of YF-12 and Orbiter "exact" (rather than equivalent) attitude responses is shown in Fig. 7, where the Orbiter amplitude characteristics have been shifted about 6 dB to take out the difference in stick gearing between the two aircraft. This comparison clearly shows that the amplitude responses are nearly identical out to a frequency of about 5.0 rad/s, as borne out also by the equivalent system characteristics in the Fig. 7 inset. These show that, aside from the gearing, the big difference is the significantly longer effective time delay of the Orbiter: τ_e is 0.264, while for the YF-12 it is only 0.093 s. Accordingly, the phase lag of the Orbiter starts rolling off at a much lower frequency, and at 4.0 rad/s has about 50 deg more phase lag than the YF-12.

The two vehicles' flight path responses to attitude, compared in Fig. 8, are nearly identical out to about 2.0 rad/s. The basic flight path lags T_{θ_2} (not noted in the figure) are similar. The differences in the higher-frequency region are, as indicated earlier, associated with the pilot's location relative to the center of instantaneous rotation (CIR) for control inputs. In the Orbiter, the pilot is aft of the CIR, giving rise to two first-order roots in the altitude response numerator. These roots, being of opposite sign and about equal magnitude, make no net phase contribution to the Orbiter response and tend to hold up the amplitude response for frequencies above 2.0 rad/s. The YF-12 pilot is forward of the CIR. The resulting roots are a lightly damped second-order pair responsible for the amplitude dip and abrupt phase lead shown in the Fig. 8 YF-12 frequency response.

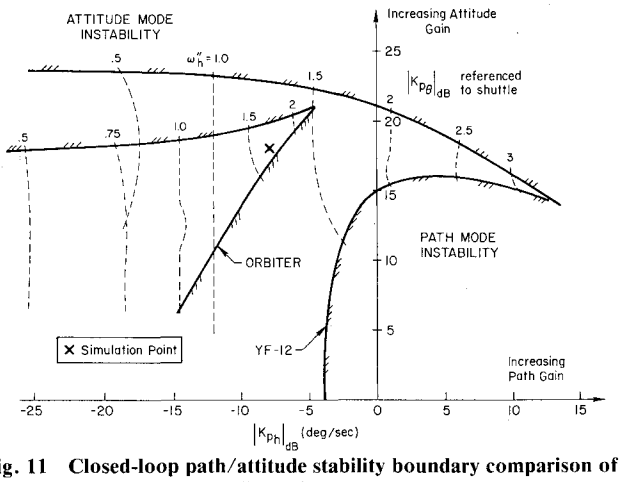

Fig. 11 Closed-loop path/attitude stability boundary comparison of YF-12 and Orbiter ALT configurations.

Pilot/Vehicle Closed-Loop Control Analyses

The YF-12 closed-loop characteristics were analyzed in the same manner as the Orbiter with the results depicted in Figs. 9-11. The root locus for the pilot's closure of the YF-12 attitude loop is shown in Fig. 9. The analogous Orbiter plot for the Fig. 9 attitude loop is Fig. 4a. A comparison of Figs. 4 and 9 shows that the YF-12 pilot has significantly higher attitude bandwidth capability. The neutral stability frequency in the

YF-12 is about 5.5 rad/s, while in the Orbiter it is slightly below 3.5 rad/s. Piloted control at the neutrally stable Orbiter closed-loop bandwidth would, in the YF-12, result in adequately damped attitude responses. The closed-loop path mode, $1/T'_{\theta_2}$, for the YF-12 (as with the Orbiter) lies very close to the bare airframe flight path lag, $1/T_{\theta_2}$.

The analogous Orbiter plots for the YF-12 outer path loop root loci of Fig. 10 were shown in Fig. 5. The pilot location zeros ω_h are clearly evident for the YF-12. The resulting path bandwidth ω_h , shown at the top of Fig. 10, of nearly 2.0 rad/s is available in the YF-12 with only modest inner-loop gain. This is about the maximum available in the Orbiter, and was achievable only with the higher inner-loop gains associated with the PIO-prone region. The lower two root loci in Fig. 10 indicate that, for tighter attitude control, the potential for a path mode instability disappears and the closed-loop path mode frequency is limited by the ω_h zeros to about 3.0 rad/s. System stability is determined only by the attitude mode.

Closed-loop path/attitude boundaries for the YF-12 are shown in Fig. 11 where the Orbiter boundaries have been superimposed for direct comparison. For YF-12 path bandwidths lower than about 1.5 rad/s, variations in attitude gain do not induce path mode instability. With attitude gains of 15-20 dB, which correspond to modest inner-loop crossover frequencies in the range of $\omega_{c_\theta} = 3.0$-4.0 rad/s, the YF-12 pilot can achieve path bandwidths of 2.0 rad/s and beyond while still retaining reasonable stability margins. Equivalent performance in the Orbiter places the pilot almost at the very tip of the stable region where the margins are near zero.

Simulation

An exploratory piloted simulation was devised to confirm that the analytically exposed differences were operationally significant. The problem was, using a fixed-base task (not normally PIO sensitive), to develop a sense of urgency and a need for fast response with the limited available display capability (a two-gun CRT), while also maintaining a reasonable approximation to a real-world approach and landing situation. A complete discussion of this development is given in Ref. 1, and an abbreviated description is given here to provide background for the results to be presented. The final display used is shown in Fig. 12. Attitude information is provided by a moving horizon relative to a fixed reference—a conventional inside-out display. Path information is provided by a "ground plane" line which moves up and down in proportion to altitude at the pilot station. The task starts with the ground plane at the bottom of the CRT screen corresponding to a wheel height of about 18 ft and a slightly nose-down pitch attitude with a corresponding positive sink rate. Once the task is started, the ground plane moves up the screen and its length shrinks to a dot at the end of 9 s. The pilot's task is to stop the ground plane on the fixed reference as smoothly as possible without overshoot before the length of the line shrinks to zero. If the pilot achieves zero h_p before the allotted time, he must try to maintain the ground contact. If the length of the line goes to zero before achieving the desired steady ground contact, it is considered analogous to stalling above the runway.

Typical Orbiter and YF-12 simulation responses, shown in Fig. 13, are quite different in nature. In the YF-12 the pilot was able to make the desired path correction quickly and smoothly and had no problem in maintaining the desired altitude; only small attitude corrections were used. In the Orbiter, large attitude excursions occurred and both attitude and altitude traces were oscillatory. Repeated trials with both aircraft consistently showed these differences. Furthermore although quite crude, measured closed-loop Orbiter frequencies (e.g., identified in Fig. 13) tend to confirm that the tight control provoked by the task corresponds quite closely to the analytically derived PIO region. This

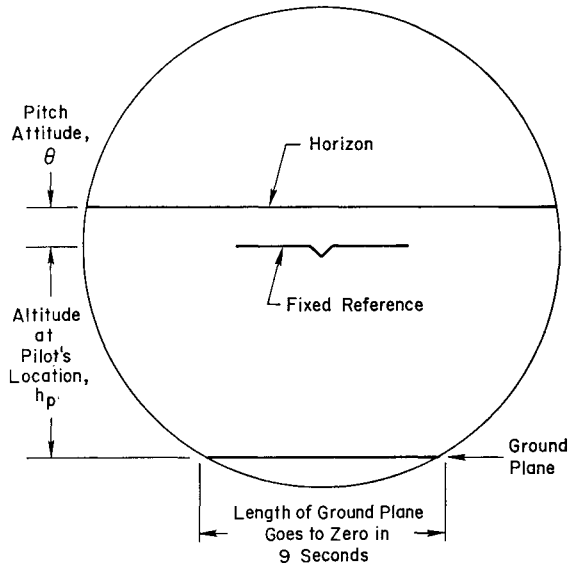

Fig. 12 Simulation display.

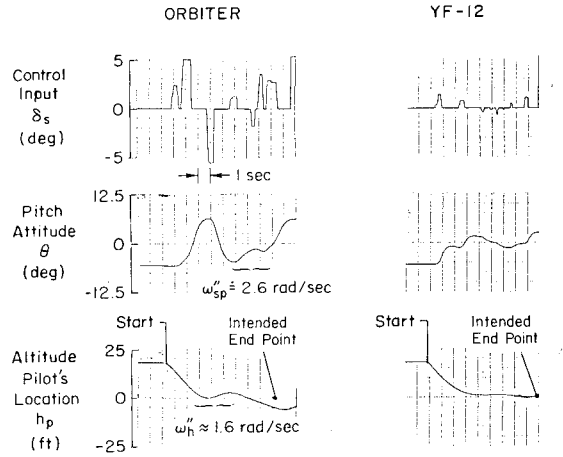

Fig. 13 Comparison of Orbiter and YF-12 simulation responses.

correspondence is shown also by plotting the simulation results as an X on the stability boundary plot of Fig 11.

Delineation and Examination of Potential Improvements

The results of the closed-loop pilot/vehicle analysis of the Orbiter and a "good" (YF-12) aircraft have been shown to be consistent with flight test and a limited fixed-base simulation designed to discriminate control capability differences. By comparing the pertinent characteristics of the two vehicles, the critical Orbiter/DFCS (digital flight control system) characteristics have been identified as: 1) excessive time delay in the attitude response to pilot control inputs, and 2) degraded path response to attitude changes associated with the unfavorable Orbiter pilot location. Because the latter characteristic is inherent in the basic vehicle geometry, our improvement efforts were devoted to correcting the first, i.e., attitude response deficiencies.

The possibilities for modifications of the Orbiter DFCS that would result in a less sluggish pitch response of the augmented Orbiter were systematically investigated. These modifications (used in various combinations) were based on the OFT (orbital flight test) rather than on the ALT configuration, the former being more appropriate in terms of future flights. However, the OFT configuration was found to offer no relief relative to the ALT.

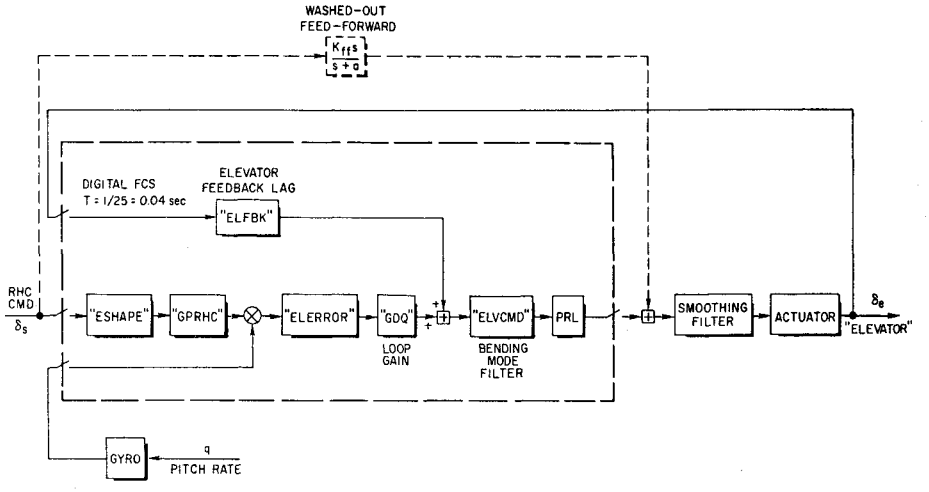

Fig. 14 Simplified OFT Orbiter/DFCS pitch channel block diagram.

Table 1 Possible improvements of Orbiter pitch response

Modification	Cumulative estimated improvement
a) More elevator feedback lag from 1.5 to 0.5 rad/s and increase loop gain (GDQ) approximately 1.5	Increase in pilot's available attitude control bandwidth from 2.35 to 3.85 rad/s
b) Add washed-out analog feed-foward from stick to actuator	Reduction in initial time delay in pitch rate response to step inputs from approximately 0.20 to 0.10 s. Further increase in available bandwidth to 5.5 rad/s
c) Move bending mode filter from forward path to pitch rate gyro feedback path	Additional reduction in initial time delay. Increase in available bandwidth

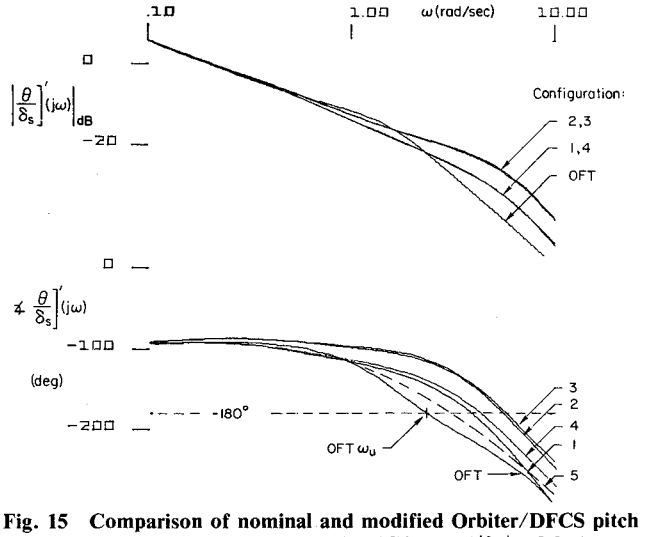

Fig. 15 Comparison of nominal and modified Orbiter/DFCS pitch attitude frequency responses for small RHC inputs ($|\delta_s| \leq 5$ deg).

The simplified OFT Orbiter/DFCS pitch channel block diagram of Fig. 14 will be used to define the modifications. (A more complete block diagram is given in Ref. 1.) The three modifications used and the corresponding estimated improvement are given in Table 1. Modification a) tightens up the basic pitch rate loop, simultaneously moving the equalization and increasing the loop gain. Modification b) attempts to overcome the initial digital delays by adding an analog path directly from the controller to the existing analog smoothing filter. This is shown by the dashed lines in Fig. 14. The practicality of this mechanization was not determined. Relocating the digital bending mode filter, modification c), could also quicken the augmented response.

The configurations simulated, made up of combinations of the above modifications, are presented as part of Fig. 16.

Pitch attitude frequency responses for the above configurations are given in Fig. 15. The effectiveness of these modifications in reducing the sluggishness of the nominal OFT pitch response can be seen in the phase characteristics of the frequency responses. These systems will subsequently be categorized by the bandwidth criterion proposed for the MIL Standard (see Ref. 9).§

Simulation Results

The Cooper-Harper ratings of the one test pilot utilized in these "blind" explorations are plotted in Fig. 16 which summarizes the main simulation results. The trend lines shown in the figure are supported by pilot commentary and further data analysis presented in Ref. 1. The ratings are plotted vs the bandwidth frequency ω_{BW} defined above.

The primary improvement is seen to arise from the analog feedforward which is common to configurations 2 and 3. Of these, configuration 3 would be the most desirable as it results in the lowest value of phase delay ($\tau_p = 0.12$).¶ Control surface rate limiting did not have an appreciable effect on the ratings for values equal to or greater than 26 deg/s. However, the rate limit of 20 deg/s is seen to result in very poor ratings at all values of bandwidths.

A "PIO suppression filter"[10] received a limited evaluation at the end of the simulation program. The exact filter mechanization is described in Ref. 1. The nonlinear filter acts directly on the RHC output and is intended to reduce the amplitude of high-frequency RHC inputs without introducing additional phase lag. The filter was used with the nominal OFT and configuation 1 with surface rate limits of 26 deg/s. In the OFT case the filter resulted in improved pilot ratings, whereas the improvement was less dramatic for configuration 1. These are shown by the "winged" symbols in Fig. 16.

All the data shown in Fig. 16 are for the defined task without additional disturbances. As described in Ref. 1,

§The bandwidth (ω_{BW}) is defined as the frequency at which the phase margin is 45 deg or the gain margin is 6 dB, whichever frequency is lower. For this experiment, phase margin set the bandwidth frequency in all cases.

¶Phase delay is an approximation to equivalent time delay and can be measured directly from the Fig. 15 frequency response plots as[9]

$$\tau_p = -[(\phi_{2\omega_{180}} + 180)/(57.3 \times 2\omega_{180})]$$

where $2\omega_{180}$ is twice the frequency where phase is -180 deg.

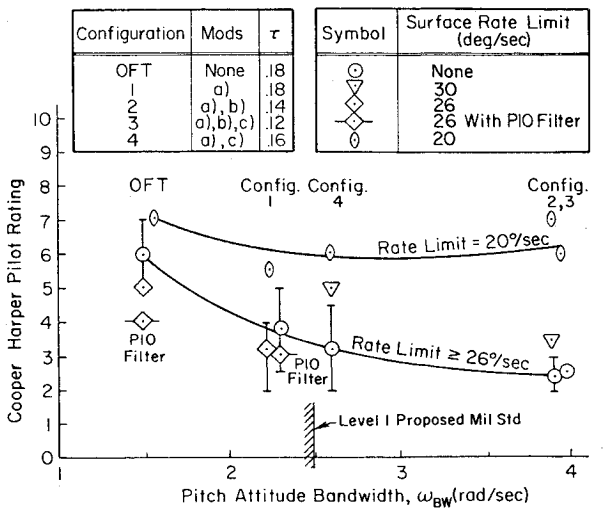

Fig. 16 Effects of bandwidth and control surface rate limiting on pilot ratings.

discrete shears were introduced to further test the configurations. The general conclusion from the trials with the shear was the obvious—task difficulty increased with the introduction and increased magnitude of the shear. The pilot commentary with the suppression filter in the presence of shears indicated some unfavorable effects centered about the pilot's inability to make rapid pitch changes when regulating against large windshears near touchdown.

Additonal, more recent results of applying the PIO suppression filter to the Shuttle Orbiter flight control system are documented in Ref. 11. This reference covers fixed-base, in-flight (125 approaches), and moving base (300 landings) simulations that selectively included discrete vertical gust disturbances and various combinations of the crosswinds and turbulence levels. The PIO tendency under high-stress conditions was considerably reduced, although an "overly aggressive control technique could still lead to a divergent PIO in some cases" for one verison of the filter and to a "loss of responsiveness" for a second version. A proper compromise between reduced PIO proneness and reduced control authority is necessary and is presumably a feature of the filter now being used on the Shuttle flights.

Conclusions

1) Analysis of the ALT-FF5 near-touchdown flight condition indicates that when the pilot needs moderately tight attitude and path control the closed-loop system is prone to pilot-induced oscillations (PIO).

2) Analysis of the Orbital flight test (OFT) configuration indicates no relief relative to the approach and landing test (ALT) configuration.

3) By comparison, a "good" aircraft (YF-12) does not show PIO-proneness for similar closed-loop bandwidths.

4) The critical Orbiter plus digital flight control system characteristics are: sluggish attitude response to stick, and degraded path response to attitude associated with unfavorable pilot location.

5) Improved attitude response alone will improve the attitude/path closed-loop stability characteristics.

6) A simple fixed-base simulation of improved systems proved consistent with analytic results, i.e., significant improvement in the pilot's ability to consistently control attitude and sink rate.

7) The configurations with the analog feedforward and tighter basic pitch loop resulted in considerable improvement (configurations 2 and 3) over the OFT.

8) The piloted simulation was strongly sensitive to imposition of the 20 deg/s surface rate limits.

6) The "PIO suppression filter" counteracted the rate limit effect when the task was flown without disturbances. Limited tests and other more recent results indicate that, depending on detailed implementation, it can reduce responsiveness, e.g., for a large windshear.

10) In the limited fixed-base experiment reported here, basic control system improvements were as effective as the PIO filter and may represent a more fundamental long-term solution to the Shuttle PIO problem. However, their implementation in an existing system would be costly in time and money, whereas the filter is a relatively simple add-on.

11) Closed-loop analysis and/or simple fixed-base simulation tasks imbued with a sense of urgency can be successfully used to predict and eliminate PIO tendencies.

Acknowledgments

The work reported in this paper was accomplished for NASA Dryden Flight Research Facility under Contract NAS4-2581, with Joseph Weil as Contract Technical Monitor.

References

[1] Teper, G.L., DiMarco, R.J., Ashkenas, I.L., and Hoh, R.H., "Analyses of Shuttle Orbiter Approach and Landing Conditions," NASA CR-163108, July 1981.

[2] "Space Shuttle Orbiter Approach and Landing Test; Final Evaluation Report," NASA, JSC-13864, Feb. 1978.

[3] "AFFTC Evaluation of the Space Shuttle Orbiter and Carrier Aircraft; NASA Approach and Landing Test," AFFTC-TR-78-14, May 1978.

[4] McRuer, D.T. and Krendel, E.S., "Mathematical Models of Human Pilot Behavior," AGARD-AG-188, Jan. 1974.

[5] van Gool, M.F.C. and Mooij, H.A., "Human Pilot Describing Function, Remnant and Associated Information for Pitch Attitude Control: Results from In-Flight and Ground-Based Tracking Experiments," National Aerospace Lab., Rept. NLR TR 75062 U, Sept. 1975.

[6] McRuer, D., Ashkenas, I., and Graham, D., *Aircraft Dynamics and Automatic Control,* Princeton University Press, Princeton, N.J., 1973.

[7] Stapleford, R.L., Craig, S.J., and Tennant, J.A., "Measurement of Pilot Describing Functions in a Single-Controller Multiloop Task," NASA CR-1238, Jan. 1969.

[8] Stapleford, R.L. and Ashkenas, I.L., "Effects of Manual Altitude Control and Other Factors on Short Period Handling Quality Requirements," AIAA Paper 65-679, 1965.

[9] Hoh, R.H., Mitchell, D.G., and Hodgkinson, J., "Bandwidth—A Criterion for Highly Augmented Airplanes," AIAA Paper 81-1890, Aug. 1981.

[10] Smith, J.W. and Edwards, J.W., "Design of a Nonlinear Adaptive Filter for Suppression of Shuttle Pilot-Induced Oscillation Tendencies," NASA TM 81349, April 1980.

[11] Powers, B.G., "An Adaptive Stick-Gain to Reduce Pilot-Induced Oscillation Tendencies," *Journal of Guidance, Control, and Dynamics,* Vol. 5, March-April 1982, pp. 138-142.

[12] Weingarten, N.C., "In-Flight Simulation of the Space Shuttle Orbiter During Landing Approach and Touchdown in the Total In-Flight Simulator (TIFS)," Calspan Corporation, Buffalo, N.Y., Rept. 6330-F-1, Sept. 1978.

[13] "Space Shuttle Orbital Flight Tests. Level C, Functional Subsystem Software Requirements. Guidance, Navigation, and Control; Part C, Flight Control-Entry," Rockwell International, Space Div., Rept. SD 76-SH-0007A, May 31, 1978.

[14] "Aerodynamic Design Data Book: Vol. I, Orbiter Vehicles; Vol. II, Mated Vehicle," Rockwell International, Space Div., Rept. SD 72-SH-0060-1G and -2G, June 1974.